

# Fabrication of Structure-Preserving Monodisperse Particles of PMMA-grafted Fullerenes

Emiko Mouri\* and Mikako Moriyama

Department of Applied Chemistry, Kyushu Institute of Technology, Kitakyushu 804-8550, Japan

(Received August 1, 2017; Revised October 6, 2017; Accepted October 17, 2017)

**Abstract:** Fullerene has fascinated characteristics and the fabrication of fullerene-containing assembly of high solubility in general solvents at facile way is immensely expected for the material processing. We aimed to control supramolecular structure of fullerene-containing molecules with arrested morphology, which would boost material potentials to wider application. In this study, we have synthesized poly(methyl methacrylate) (PMMA)-grafted fullerene and the association behavior of PMMA-grafted fullerene in solvent is utilized to obtain monodisperse assemblies with submicron size. Furthermore, we have succeeded to fix the assembly morphology by UV irradiation and recovered the assembly in another solvent in which the assembly basically does not form. This procedure enables us to obtain fullerene-dispersed materials at sub- $\mu\text{m}$  order with various matrixes.

**Keywords:** Polymer-grafted fullerene, Assembly, UV irradiation, Fullerene, PMMA, Micelle

## Introduction

Fullerene ( $C_{60}$ ) is one of the most attractive materials in nanomaterial science due to its specific shape and versatile characteristics like semiconducting, high thermal stability, high refractive index, high heat conductivity, radical trapping properties, etc. [1-5]. Important issues behinds the application of fullerene in material science and biological science have been a low solubility or miscibility of fullerene in general solvents or polymer matrixes.

The general way to overcome the problem of low solubility is to modify  $C_{60}$  by functional groups [6] or polymer component [7]. Alternatively, complex formation with surfactants [8] or polymer [9] is also utilized in addition to charge-transfer complex formation [10]. In the last two decades, many  $C_{60}$ -derivatives have been synthesized mostly aiming at higher solubility in a universal solvent [1-5]. Polymer-grafted fullerenes also have been synthesized including very sophisticated systems [7,11-32] in which fullerene solubility can be controlled drastically by one (or two) long chain for one fullerene molecule keeping conjugated nature of fullerene. Yashima *et al.* approached this problem from another side to synthesize PMMA-grafted  $C_{60}$  with controlled tacticity of PMMA [29]. They showed that  $C_{60}$  molecules can be captured by PMMA helix [33], which would be one of the most sophisticated ways to increase miscibility of  $C_{60}$ , and the superstructure is also constructed [34].

On the basis of the synthetic modification of fullerene, further investigation on the association behavior of fullerene-containing molecules beyond the molecular order captures enormous attention [3]. One of the promising application candidates for polymer-grafted fullerene is the organic solar cell device [32,35] due to the high potential of fullerene as

an electron acceptor. The control of the morphology of polymer-grafted fullerene is a key to obtain high energy conversion. The fabrication of fullerene-containing assembly of high miscibility and stability at facile way is immensely expected for the material processing. The association behavior of the polymer-modified fullerene has been studied although the numbers of the studies are not so large [11,12,21-28]. The size of their assemblies usually exceeds 100 nm in poly(ethylene oxide) [22], poly(methacrylic acid) [25], poly(methyl methacrylate) [26], and poly(acrylic acid) [27] systems while micelles with 3-5 nm hydrodynamic radius were observed in systems containing poly[2-(dimethylamino)-ethyl methacrylate] system [23]. In poly(*t*-butyl methacrylate) system, vesicular aggregates are found [24]. Although we do not have a complete picture of association behavior of polymer grafted fullerene system from the former studies, we suppose that the observed large aggregation should be attributed to a strong adhesion force between  $C_{60}$ .

The association behavior in solvent would be affected by polymer molecular weight, solvent, and temperature not just by polymer species. This sensitivity would be a drawback for material processing. Controlling supramolecular structure of fullerene-containing molecules with arrested morphology would boost material potentials to wider application. Aiming at fabrication of  $C_{60}$ -polymer composite with preserved nanostructure in any solvent or matrix, we focused on the fabrication of PMMA-grafted fullerene assembly in this paper. PMMA is one of the general polymers and is used in versatile fields. By adding fullerene component to PMMA, improved optical refractivity and thermal stability of the materials are expected [9,31]. Tam *et al.* [3] would be one of the pioneering groups to investigate polymer grafted fullerene association behavior using well-defined polymer via ATRP (Atomic Transfer Radical Polymerization) in which the atom transfer step is the key step in the reaction responsible for uniform polymer chain growth. They reported on PMMA-

\*Corresponding author: mouri@che.kyutech.ac.jp

grafted fullerene and they showed us that the large assembly more than 100 nm was observed in acetate/decaline solvent mixture [26]. The large assembly is considered to be large compound micelle (LCM) [36,37].

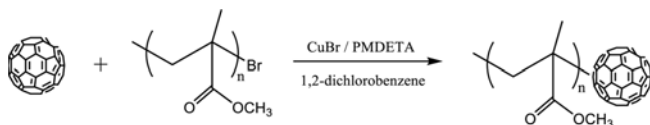
In this paper, we report that we have synthesized PMMA-grafted fullerene and investigate the association behavior through UV (ultra-violet) light irradiation to the assembly. We have found that ca. 250-nm sized assemblies are formed in a selective solvent for PMMA with high monodisperse nature and the morphology of the assemblies can be preserved by the UV irradiation to the solution. We can recover the ca. 250-nm sized assemblies in the different solvent in which PMMA- $C_{60}$  does not form assemblies without UV irradiation. The molecular weight of PMMA shows an effect on assembly size in the solvent and too large PMMA is not appropriate to preserve the assembly structure.

## Experimental

### Synthesis of PMMA-grafted Fullerene

As a first step of synthesizing PMMA-grafted fullerene, PMMA homopolymer is synthesized by ATRP. In the testing tube, freshly distilled MMA monomer (Kanto Chemical Co., Inc., Tokyo, Japan), ATRP initiator of 2-bromo-2-methylpropionic acid (Aldrich, United States),  $N,N,N',N'',N''$ -pentamethyldiethylenetriamine (PMDETA) (Kanto Chemical Co., Inc., Tokyo, Japan) and CuBr(I) (Wako Chemical, Osaka, Japan) were mixed in anisole. Typical feed is 3 ml of dry MMA, 50 mg of 2-bromo-2-methylpropionic acid, 20 mg of CuBr, and 125 mg of PMDETA in 2 ml of dry anisole. The mixture was carefully degassed with four or five freezing-pump-thaw cycles, then, the ample was sealed off completely under vacuum. The polymerization was carried out at 50-60 °C for 1.5-3 h depending on the molecular weight of PMMA (Table S1). The reaction conversion is ranged from 23.6 % to 46.5 % depending on the sample. After the reaction the solution of reactant was purified by aluminum column. PMMA was obtained by re-precipitation by methanol. Obtained polymer samples were characterized by  $^1\text{H-NMR}$  (proton nuclear magnetic resonance) and GPC (gel permeation chromatography).

In the second step, the reaction of Br-terminated PMMA and fullerene (Fullerene, nano purple st 98 %, Frontier carbon, Fukuoka, Japan) was conducted. In this reaction as shown in Scheme 1, Br-terminated PMMA was used as an initiator. The initiator, CuBr, PMDETA and fullerene were mixed in the testing tube with 1,2-dichlorobenzene as a



**Scheme 1.** Reaction scheme for synthesizing PMMA- $C_{60}$ .

solvent and reacted at 90 °C for 24 h with  $N_2$  atmosphere. Fullerene was fed three times larger compared to PMMA. The reactant was purified by aluminum column with THF and silica column with chloroform to remove Cu species and unreacted fullerene, respectively. The samples were obtained through re-precipitation by methanol.

### Characterization of PMMA-grafted Fullerene

The characterization of PMMA-grafted fullerene was performed by  $^1\text{H-NMR}$  (400 MHz,  $\text{CDCl}_3$ ) (AVANCE-400, Bruker, USA),  $^{13}\text{C-NMR}$  (125 MHz,  $\text{CDCl}_3$ ) (JNM-A500, JEOL, Tokyo, Japan), GPC equipped with column oven (CTO-10A/10AC, Shimadzu, Kyoto, Japan) and refractive index detector (RI153, JASCO Corp., Tokyo, Japan). We

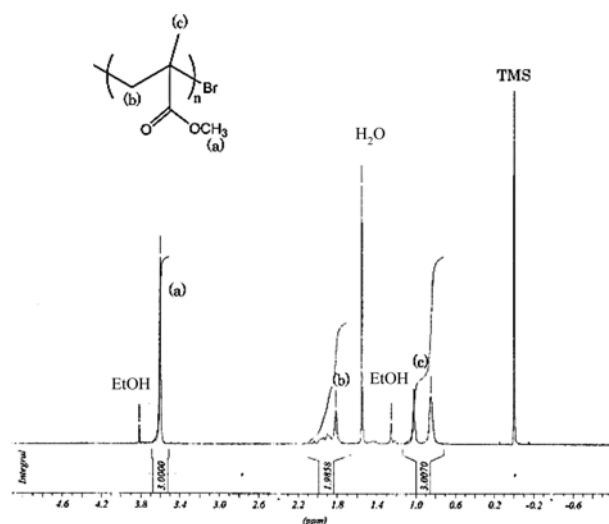


**Figure 1.**  $^1\text{H-NMR}$  spectrum for PMMA in  $\text{CDCl}_3$ .

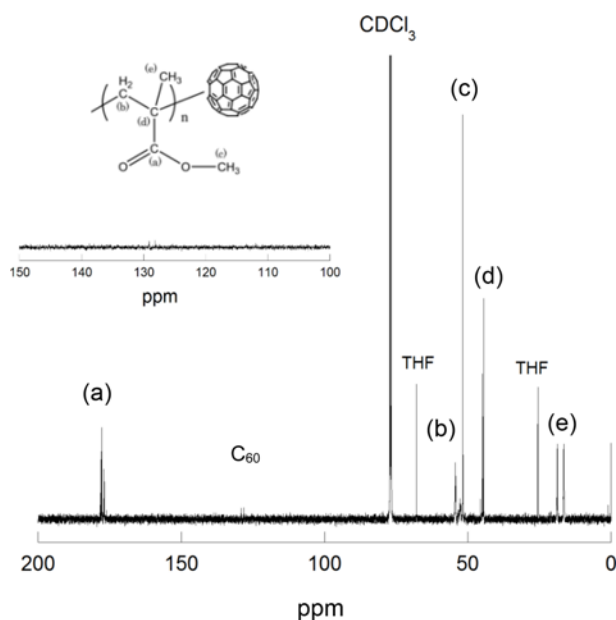


**Figure 2.**  $^{13}\text{C-NMR}$  spectrum for PMMA- $C_{60}$  in  $\text{CDCl}_3$ .

also analyzed samples by TGA (thermo gravimetry analysis) (TGA-50, Shimadzu, Kyoto, Japan). We confirmed that the PMMA was synthesized by  $^1\text{H-NMR}$  (Figure 1), and that  $\text{C}_{60}$  is included in the sample by  $^{13}\text{C-NMR}$  (Figure 2). TGA measurement was conducted from room temperature to 600 °C to obtain  $\text{C}_{60}$ : PMMA ratio in samples. From TGA and GPC data, we estimated the constituent of samples.

### Size Estimation of Self-Assemblies

PMMA- $\text{C}_{60}$  samples were dissolved in filtered acetonitrile and chloroform at 0.2 wt%, respectively, and exposed to ultrasonication for 24 h before DLS (dynamic light scattering) measurement. Acetonitrile is selective solvent for PMMA, and chloroform dissolves both components well. DLS measurement was performed by DLS-7000 (Otsuka Electronics Co., Ltd., Hirakata, Japan) with a He-Ne laser (632.8 nm wavelength) at 90° scattering angle at 25 °C. We obtained the time correlation function,  $g^2(\tau)$ , of the measured scattered intensity defined by the following equation:

$$g^2(\tau) = \frac{\langle I(t)I(t+\tau) \rangle}{\langle I(t) \rangle^2}$$

where  $I(t)$  is the scattered intensity at time  $t$ , and  $\tau$  is the delay time. We employed the plots of  $g^2(\tau)-1$  against  $\tau$  because the time correlation function of scattered amplitude,  $g^1(\tau)$ , is related to  $g^2(\tau)$  by the following equation:

$$g^2(\tau) - 1 = \beta |g^1(\tau)|^2$$

where  $\beta$  is the coherent factor. Data analysis was carried out by the curve fitting of time-correlation function of scattering intensity to exponential function. CONTIN analysis was also performed in addition to exponential fitting. In the data analysis, we use scattering intensity-based fraction throughout the investigation, not the number-based fraction or volume-based fraction.

We obtained hydrodynamic diameter based on translational diffusion constant from the curve fitting with an exponential function and Stokes-Einstein equation. The values for diffractive indexes 1.344 and 1.443 were used for acetonitrile and chloroform, respectively. The values for viscosities 0.34 mPa·s and 0.53 mPa·s were used for acetonitrile and chloroform, respectively. In addition to DLS measurement, the morphology of dried PMMA- $\text{C}_{60}$  assembly was observed by TEM (H-7650, Hitachi, Tokyo, Japan).

### UV Irradiation to PMMA- $\text{C}_{60}$ Assembly

PMMA- $\text{C}_{60}$  assemblies formed in acetonitrile were subjected to UV irradiation aiming at arresting the morphology. In the test tube, PMMA- $\text{C}_{60}$  acetonitrile solution (0.2 wt%, ca. 3 ml) was degassed and filled with nitrogen several times repeatedly and irradiated by super-high-pressure mercury lamp (SX-UI500H, USHIO Inc., Tokyo, Japan) for 12 h. After the UV irradiation, acetonitrile was removed by

evaporation and added 3 ml of chloroform. DLS measurement was conducted for the samples after 6 h ultra sonification of the chloroform dispersion using BRANSONIC® ultrasonic cleaner (1510J-MT, Emerson, Ltd., St. Louis, U.S.) to accelerates re-dispersion. In addition to DLS measurement, the morphology of cross-linked PMMA- $\text{C}_{60}$  assembly was observed by TEM (H-7650, Hitachi, Tokyo, Japan). The characteristic change through the irradiation was examined by IR measurement (JIR-5500, JASCO Corp., Tokyo, Japan).

## Results and Discussion

We synthesized three samples of PMMA-grafted  $\text{C}_{60}$  with different molecular weights of PMMA. Figure 1 is representative  $^1\text{H-NMR}$  of PMMA.  $^1\text{H-NMR}$  ( $\text{CDCl}_3$ , 400 MHz) for PMMA;  $\delta$ : 0.7-1.1 (m,  $\text{CH}_3$ ), 1.7-2.1 (m,  $\text{CH}_2$ ), 3.67 (m,  $\text{OCH}_3$ ) ppm. Synthesized PMMA has number-averaged molecular weight ranged from 22,000 to 41,000 with relatively narrow distribution as in Table 1 by GPC. By using these homopolymers, we conducted the reaction to  $\text{C}_{60}$ . We confirmed the removal of unreacted  $\text{C}_{60}$  by column treatment based on TLC (thin layer chromatography). After the free  $\text{C}_{60}$  removal, we measured  $^{13}\text{C-NMR}$  in which the peaks characteristics to modified  $\text{C}_{60}$  around 130 ppm were confirmed. Figure 2 is representative  $^{13}\text{C-NMR}$  of PMMA- $\text{C}_{60}$ .  $^{13}\text{C-NMR}$  ( $\text{CDCl}_3$ , 125 MHz) for PMMA- $\text{C}_{60}$ ;  $\delta$ : 19-16 (m,  $\text{CH}_3$ ), 44-46 (m, C), 51-52 (m,  $\text{OCH}_3$ ), 53-55 (m,  $\text{CH}_2$ ), 127-129 (m,  $\text{C}_{60}$ ), 175-178 (m, C=O) ppm.

For further characterization, TGA analysis was performed. TGA curves of PMMA- $\text{C}_{60}$  shown in Figure 3 are not the simple summation of curves for PMMA and fullerene. (Representative PMMA curves are shown in many literatures [38] and shows smooth decrease around 400-450 °C.) The TGA curves for PMMA- $\text{C}_{60}$  indicate higher thermal stability and the shape of the curves depends on the molecular weight of grafted PMMA. The differential curves (Figure S1) also indicate the clear shift of the peak to the higher temperature. The similar tendency is also shown in the study by Pereira *et al.* in which fullerene is mixed with PMMA [39]. By introducing fullerenes to PMMA, the thermal stability is considered to be elevated also in our system. The difference in TGA curves between PMMA22k- $\text{C}_{60}$  and PMMA31k- $\text{C}_{60}$  cannot be fully explained just by the fullerene fraction, some kind of microstructure of the samples might affect the TGA curves.

**Table 1.** Characteristics of PMMA- $\text{C}_{60}$  samples

Sample code	$M_n$	$M_w/M_n$	PMMA (wt%)	$\text{C}_{60}$ (wt%)
PMMA- $\text{C}_{60}$ -22k	22,000	1.45	99.35	1.65
PMMA- $\text{C}_{60}$ -31k	31,000	1.22	99.65	0.35
PMMA- $\text{C}_{60}$ -41k	41,000	1.19	99.45	0.55

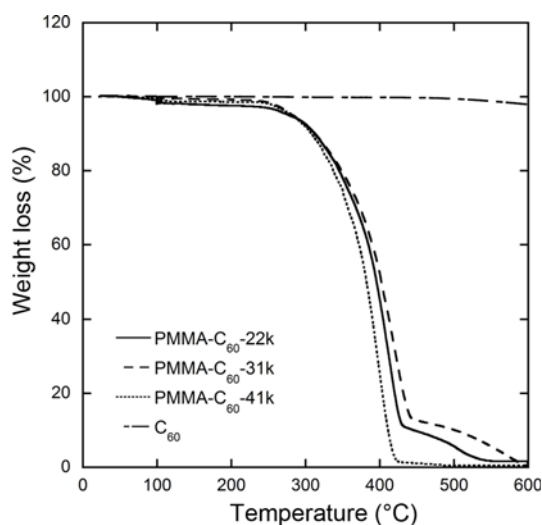
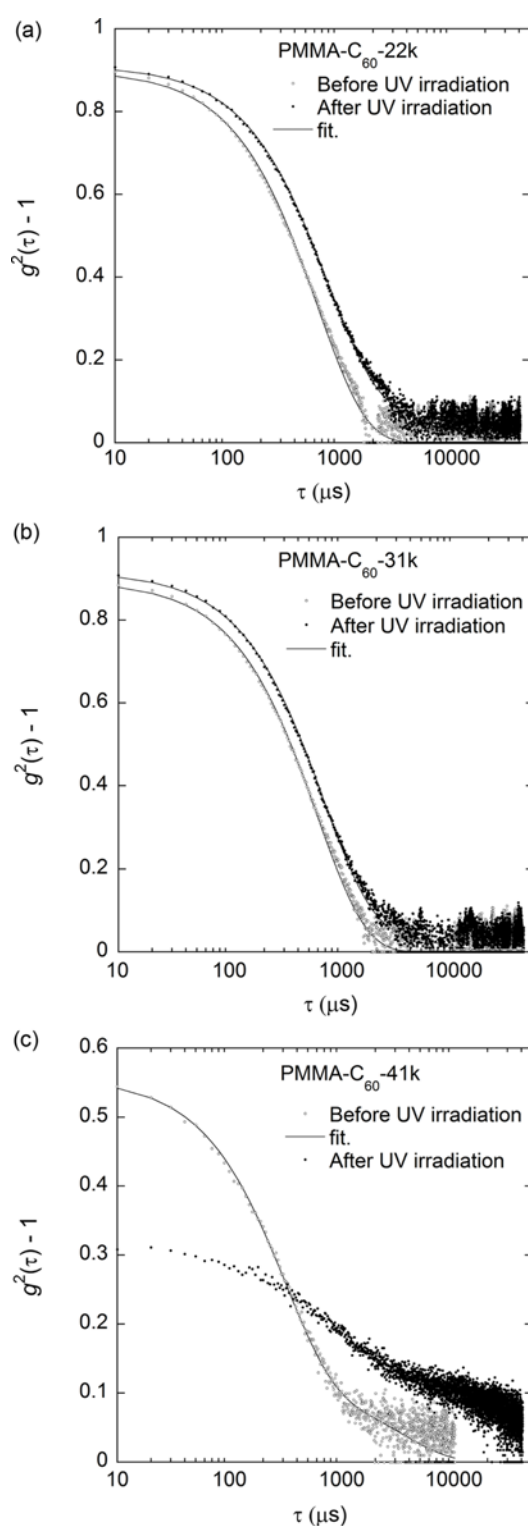


**Figure 3.** TGA curves for three PMMA-C<sub>60</sub> samples.

We also estimated the fraction of C<sub>60</sub> and PMMA in each sample by TGA analysis (Figure 3, Table 1) although we could not confirm the complete removal of uncapped PMMA due to the difficulty in distinguishing free PMMA and PMMA-C<sub>60</sub> by GPC or TLC etc. By using these TGA curves, we calculated that samples contain PMMA than 98.3-99.6 wt% in weight basis. The contents of C<sub>60</sub> indicated in Table 1 are rather smaller than calculated values from molecular weight from GPC: Calculated values of C<sub>60</sub> content are 2.2-1.4 wt% base on weight-averaged molecular weight. Comparing with former study of PMMA-grafted fullerene [26], our samples have larger molecular weight of PMMA and this sample composition makes it difficult to characterize PMMA-C<sub>60</sub>. We basically regard that PMMA-C<sub>60</sub> is successfully obtained although we still have the possibility that the samples contain uncapped PMMA.

In the next stage, we dissolved PMMA-C<sub>60</sub> samples to solvents attempting micelle formation. We tested several solvents to choose the right solvent in micelle formation, and we choose acetonitrile expecting PMMA-C<sub>60</sub> to form micelle-like assembly because acetonitrile can solvate PMMA while it does not solvate C<sub>60</sub>. On the other hand, chloroform was chosen to be a control solvent to see the difference: Both PMMA and C<sub>60</sub> can be solubilized in chloroform.

We confirmed micelle formation of PMMA-C<sub>60</sub> by DLS measurement. Figure 4 shows time-correlation function obtained by DLS measurements, and the time-correlation function was fitted with single exponential function or double exponential function to obtain hydrodynamic radius based on Einstein-Stokes equation. The obtained hydrodynamic diameters for three samples are in Table 2 with their fractions in scattering intensity. Two samples with smaller molecular weight PMMA-22k-C<sub>60</sub> and PMMA-31k-C<sub>60</sub> form monodispersed assembly with 270-290 nm diameters, while a sample with larger molecular weight PMMA-41k-C<sub>60</sub> forms

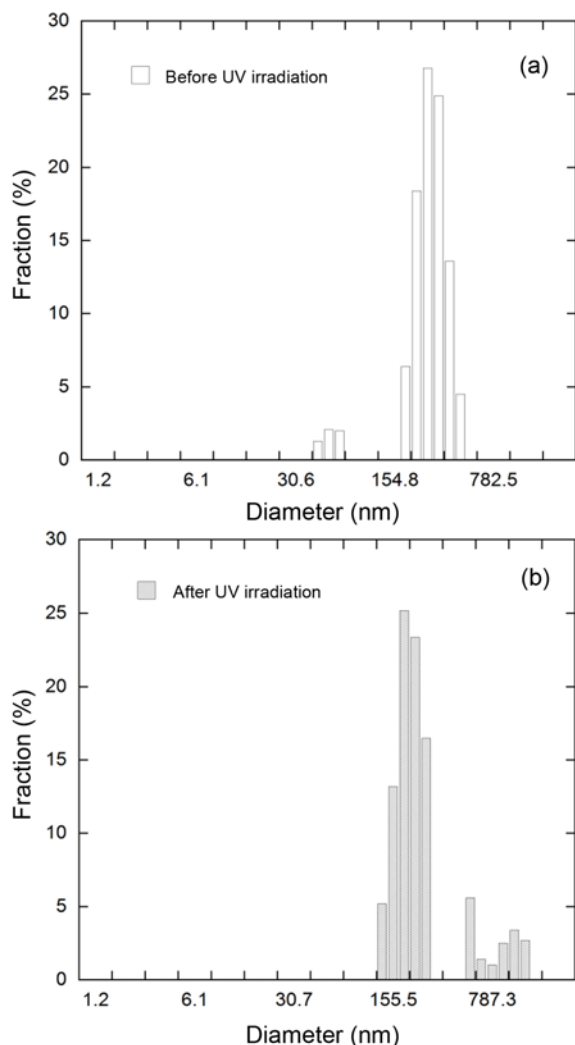


**Figure 4.** Time-correlation functions ( $g^2(\tau)-1$ ) obtained from DLS measurement for (a) PMMA-C<sub>60</sub>-22k, (b) PMMA-C<sub>60</sub>-31k, and (c) PMMA-C<sub>60</sub>-41k. Measurements were carried out in acetonitrile before UV irradiation and in chloroform after UV irradiation. The lines are most fitted exponential curves calculated with the parameters in Table 2.

**Table 2.** Hydrodynamic diameters of assembly formed by PMMA-C<sub>60</sub>

Sample code	Before UV irradiation Diameter (nm)	After UV irradiation Diameter (nm)
PMMA-C <sub>60</sub> -22k	290	260 (0.87), 2300 (0.13)
PMMA-C <sub>60</sub> -31k	270	230 (0.93), 2100 (0.07)
PMMA-C <sub>60</sub> -41k	140 (0.8), 1600 (0.2)	Large aggregates

The number in the parentheses is scattering-intensity-based fraction which means the fraction contributed to time correlation function.

**Figure 5.** Particle size distribution analyzed by CONTIN method for PMMA-C<sub>60</sub>-31k assembly (a) before and (b) after UV irradiation.

a smaller sized assembly with 140 nm diameter with larger aggregates in  $\mu\text{m}$  order.

Especially for the two samples with lower PMMA molecular weight, the monodisperse nature of these assemblies is remarkable, which is supported by high reproducibility of the DLS curves by single exponential function. However,

the diameter of about 270-290 nm is much larger than reasonable micelle size which is supposed to be ca. 10 nm. By CONTIN analysis shown in Figure 5, we found small fraction at a diameter of 10-nm order (ca. 40-60 nm), which might be attributed to small aggregation of PMMA-C<sub>60</sub> micelles. (In the data analysis, we use scattering intensity-based fraction throughout the investigation.) This micelle size estimation is based on PMMA chain length and C<sub>60</sub> size assuming based that PMMA chains behave like Gaussian chains. For a monodisperse large assembly with submicron size, it is reasonable to suppose some kinds of principle control the organized structure of a few hundred nm sized monodisperse assembly because general aggregate does not show this kind of high monodisperse nature. Ravi *et al.* previously reported similar result in a different solvent and they propose porous-like large compound micelles (LCM) [26]. LCM is the hierarchical assembly formed by spherical micelles, which is originally proposed by Eisenberg *et al.* for the assembly formed by amphiphilic polymer [36,37]. We suppose that LCM is also formed in our system as supported by TEM in the following section.

We further treat the assemblies to keep the assembly morphology in the solvent to enable us to obtain the monodisperse fullerene-containing particle in various circumstances. If you can preserve the assembly morphology, it enables us to re-disperse the ca. 250-nm sized assemblies in more various solvents and polymer matrixes regardless of the interaction between fullerene moiety and solvents or matrixes. For this purpose, we tried to cross-link the core part through radical reaction by UV irradiation to the dispersion of PMMA-C<sub>60</sub> assembly. The reaction between fullerene molecules to fabricate poly(fullerene)s by UV irradiation are reported by many authors [40,41]. In the reported paper, a [2+2] cycloaddition reaction mechanism has been proposed for the photopolymerization process [40,41]. In our case, fullerene moiety would be segregated from PMMA moiety in the assembly; high partial concentration of C<sub>60</sub> can accelerate the photoreaction.

The dispersion after the irradiation is dried and the samples are re-dispersed in chloroform which solves both PMMA and C<sub>60</sub>. In Figure 4, DLS data taken for samples in chloroform after UV irradiation is also presented. The DLS data shows that the existence of assembly by PMMA-C<sub>60</sub> was confirmed irrespective of PMMA molecular weight after UV irradiation. As shown in Table 2, assembly size was almost preserved by the procedure especially for the two samples with the smaller molecular weight of PMMA. For PMMA-C<sub>60</sub>-22k and PMMA-C<sub>60</sub>-31k, original-sized assembly was almost preserved although the formation of larger aggregates is slightly confirmed. The fraction shown in Table 2 is the scattering intensity-based fraction which estimates larger for larger-sized aggregates compared to number-based fraction. CONTIN analysis of DLS data also supports the same trend in Figure 5. Thus, the fraction of the

aggregates at number basis is extremely small: assembly of submicron size is maintained through UV irradiation and solvent exchange.

For the PMMA-C<sub>60</sub>-41k sample, large assembly formation beyond DLS measurement limit was found, which is obvious from the drastic change of time correlation function obtained by DLS measurements in Figure 4. The curve fitting with two exponential within measurement limiting size was unable in this case. On the other hand, we confirmed that no assembly or aggregation was found in a chloroform solution of PMMA-C<sub>60</sub> without UV irradiation, which is reasonable to reflect that both PMMA and C<sub>60</sub> can dissolve in chloroform.

Much difference was observed in assembly size after UV irradiation depending on the molecular weight of PMMA. For the samples with smaller PMMA molecular weight, assembly formation of similar size as before the irradiation was found in chloroform. This implies that the photoreaction only occurs in micelle core. On the other hand, aggregation occurred in the sample with large PMMA sample. One possible scenario is that the photoreaction occurs between fullerenes in different assemblies. This might induce aggregation of a submicron assembly to form larger aggregates. This can be rationalized by the fact that smaller assemblies are formed for PMMA-C<sub>60</sub>-41k before irradiation: Photoreaction between fullerenes belongs to different assemblies more likely occur with smaller assemblies, i.e., with a larger specific surface area.

We also confirmed the assembly morphology before and after UV irradiation by TEM, which is shown in Figure 6. TEM image before the UV irradiation shows monodisperse particles with ca.150 nm diameter. From the TEM image, we can see that the 150-nm sized particle is composed of sub-particles with smaller diameter around 20 nm, although the outlines of the sub-particles are not so clear. The sub-particle size is relatively reasonable size as a micelle; we suppose that micelles compose the sub-micron particle as building blocks. This is also supported by the former study by Ravi *et al.* in which PMMA-grafted fullerene forms assemblies with ca.100 nm diameters in ethyl acetate/decaline mixture solvent and they suppose that the assembly is composed of spherical micelle with 10-20 nm diameter [26]. Their finding is limited to PMMA-C<sub>60</sub> sample with single molecular weight sample in acetate/decaline mixture solvent, our result rationalizes that this association behavior is more general in wider molecular weight range and solvent.

After the irradiation, similar morphology to the one before the irradiation was confirmed as in Figure 6(b), and we can confirm that the morphology was principally preserved. The size difference obtained by TEM and DLS may arise by the different status of samples: Dried samples are used in TEM observation while dispersions are used for DLS measurements. We suppose that the drying process shrinks up the PMMA-C<sub>60</sub> assembly. For the large M<sub>n</sub> of PMMA sample, a non-

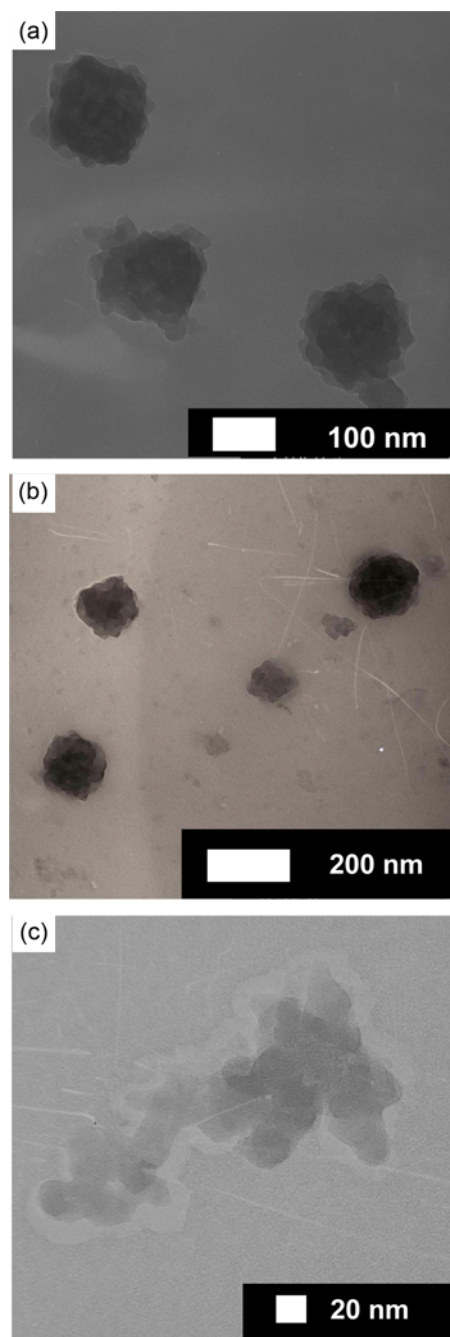


**Figure 6.** TEM images for PMMA-C<sub>60</sub>-31k (a) before UV irradiation and (b) after UV irradiation. (c) Non-spherical aggregation obtained after UV irradiation for PMMA-C<sub>60</sub>-41k.

spherical shaped particle is obtained by TEM (Figure 6(c)). In Figure 6(c), non-spherical aggregate formed by smaller blocks around 20 nm is observed. This kind of irregular shape may affect the DLS results. Thus, at a limited range of molecular weight of PMMA, we successfully fabricated monodisperse fullerene containing assembly. Figure 7 shows schematic process for the fabrication of structure-preserving

fullerene-containing assembly. In the first stage, assemblies are formed in selective solvent, and the second stage, the sample solution was subjected to UV irradiation. In the last stage, the assemblies at preserved structure are recovered in general solvent. We have confirmed the structural preservation by DLS and TEM. However, we do not have an exact proof for the photoreaction in the assemblies. We can apply this process for other systems containing fullerenes by clarifying the photoreaction process in the near future.

The change in component by the UV irradiation was examined by IR spectra measurements. Figure 8 shows IR spectra of PMMA-C<sub>60</sub> samples before and after UV irradiation. The infrared spectrum of C<sub>60</sub> consists of four modes observed at frequencies of 527, 576, 1182 and 1429 cm<sup>-1</sup>. The 527 and 576 cm<sup>-1</sup> modes are associated with a primarily radial motion of the carbon atoms, while the 1182 and 1427 cm<sup>-1</sup> modes are essentially associated with a tangential motion of the carbon atoms [42]. These four frequency ranges are overlapped with PMMA spectrum and we cannot see clear peaks derived from C<sub>60</sub> in Figure 6. However, the largest difference between the two spectra is

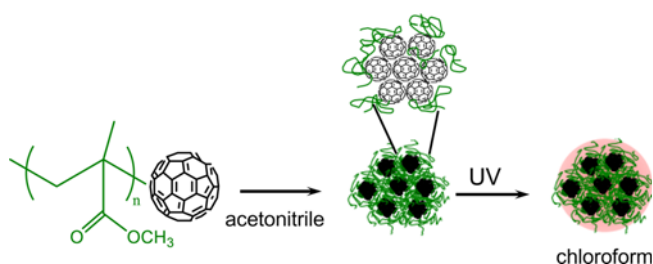


**Figure 7.** Schematic presentation of the fabrication process of PMMA-C<sub>60</sub> monodisperse assembly.

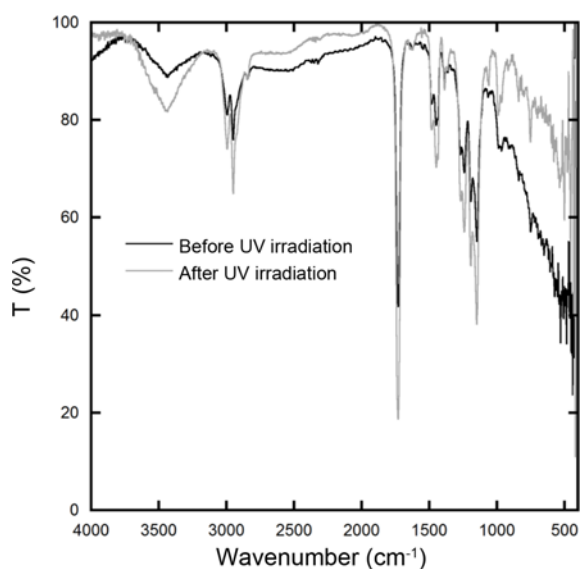


**Figure 8.** IR spectra of PMMA-C<sub>60</sub>-31k before and after UV irradiation.

found in the wavenumber range below 1000 nm<sup>-1</sup>. In this range, absorption was largely decreased by the UV irradiation, which raises the possibility that adsorption at 527 and 576 cm<sup>-1</sup> are depressed by UV irradiation. IR spectra change suggests that the change in a component surely occurs in addition to the dispersion property change confirmed by DLS.

## Conclusion

We have demonstrated the fabrication of submicron-sized fullerene containing monodisperse assembly by PMMA-grafted fullerene. Assemblies formed in acetonitrile can be re-dispersed in chloroform with fixed morphology through UV irradiation. The molecular weight of PMMA shows an effect on assembly size and too large PMMA is not appropriate to fix the assembly. By this procedure, fullerene-containing assemblies can be redispersed in a versatile organic solvent, which opens the way to a wider application.

## Acknowledgements

We are greatly thankful to Prof. Kohji Yoshinaga (Professor Emeritus of Kyushu Institute of Technology) for his advice in the experiments especially for the synthesis of the samples. E.M. appreciates kind advice from Dr. Tsuyoshi Takakura (Mitsubishi Chemical). We also thank the assistance of Mr. Masumi Kunisue for the NMR measurements. This work was financially supported by a grant-in-aid (No. 19750099, 24850015) from JSPS.

**Electronic Supplementary Material (ESM)** The online version of this article (doi: 10.1007/s12221-017-7663-0) contains supplementary material, which is available to authorized users.

## References

1. F. Giacalone and N. Martin, *Chem. Rev.*, **106**, 5136 (2006).
2. K. Ariga, T. Nakanishi, and J. P. Hill, *Curr. Opin. Colloid Interface Sci.*, **12**, 106 (2007).
3. P. Ravi, S. Dai, C. Wang, and K. C. Tam, *J. Nanosci. Nanotech.*, **7**, 1176 (2007).
4. E.-Y. Zhang and C.-R. Wang, *Curr. Opin. Colloid Interface Sci.*, **14**, 148 (2009).
5. Y. Zhao and G. Chen, *Struct. Bond.*, **159**, 23 (2014).
6. L. Y. Chiang, J. B. Bhonsle, L. Wang, S. F. Shu, T. M. Chang, and J. R. Hwu, *Tetrahedron*, **52**, 4963 (1996).
7. H. Okamura, T. Terauchi, M. Minoda, T. Fukuda, and K. Komatsu, *Macromolecules*, **30**, 5279 (1997).
8. K. C. Hwang and D. Mauzerall, *J. Am. Chem. Soc.*, **114**, 9705 (1992).
9. K. Yoshinaga, S. Motokucho, K. Kojio, and A. Nakai, *Colloid. Polym. Sci.*, **290**, 1221 (2012).

10. D. V. Konarev and R. N. Lyubovskaya, *Rus. Chem. Rev.*, **68**, 1938 (1999).
11. H. Okamura, N. Ide, M. Minoda, K. Komatsu, and T. Fukuda, *Macromolecules*, **31**, 1859 (1998).
12. X. Wang, S. H. Goh, Z. H. Lu, S. Y. Lee, and C. Wu, *Macromolecules*, **32**, 2786 (1999).
13. P. Zhou, G. Q. Chen, H. Hong, F. S. Du, Z. C. Li, and F. M. Li, *Macromolecules*, **33**, 1948 (2000).
14. W. T. Ford, T. Nishioka, S. C. McCleskey, T. H. Mourey, and P. Kahol, *Macromolecules*, **33**, 2413 (2000).
15. X. D. Huang and S. H. Goh, *Macromolecules*, **33**, 8894 (2000).
16. L. Li, C. Wang, Z. Long, and S. J. Fu, *J. Polym. Sci., Part A: Polym. Chem.*, **38**, 4519 (2000).
17. X. D. Huang, S. H. Goh, and S. Y. Lee, *Macromol. Chem. Phys.*, **201**, 2660 (2000).
18. X. D. Huang and S. H. Goh, *Polymer*, **43**, 1417 (2002).
19. T. Song, S. H. Goh, and S. Y. Lee, *Macromolecules*, **35**, 4133 (2002).
20. J. Yang, L. Li, and C. Wang, *Macromolecules*, **36**, 6060 (2003).
21. T. Song, S. Dai, K. C. Tam, S. Y. Lee, and S. H. Goh, *Polymer*, **44**, 2529 (2003).
22. T. Song, S. Dai, K. C. Tam, S. Y. Lee, and S. H. Goh, *Langmuir*, **19**, 4798 (2003).
23. S. Dai, P. Ravi, C. H. Tan, and K. C. Tam, *Langmuir*, **20**, 8569 (2004).
24. C. H. Tan, P. Ravi, S. Dai, K. C. Tam, and L. H. Gan, *Langmuir*, **20**, 9882 (2004).
25. P. Ravi, S. Dai, C. H. Tan, and K. C. Tam, *Macromolecules*, **38**, 933 (2005).
26. P. Ravi, S. Dai, K. M. Hong, K. C. Tam, and L. H. Gan, *Polymer*, **46**, 4714 (2005).
27. C. Wang, P. Ravi, and K. C. Tam, *Langmuir*, **22**, 2927 (2006).
28. H. Yu, L. H. Gan, X. Hu, and Y. Y. Gan, *Polymer*, **48**, 2312 (2007).
29. T. Kawaguchi, J. Kumaki, and E. Yashima, *J. Am. Chem. Soc.*, **127**, 9950 (2005).
30. H. Wakai, T. Momoi, T. Shinno, T. Yamaudhi, and N. Tsubokawa, *Mater. Chem. Phys.*, **118**, 142 (2009).
31. R. Katiyar, D. S. Bag, and I. Nigam, *Thermochem Acta*, **557**, 55 (2013).
32. F. Pierini, M. Lanzi, P. Nakielski, S. Pawlowska, O. Urbanek, K. Zembrzycki, and T. A. Kowalewski, *Macromolecules*, **50**, 4972 (2017).
33. T. Sugai, H. Shinohara, and E. Yashima, *Angew. Chem., Int. Ed.*, **47**, 515 (2008).
34. N. Ousaka, F. Mamiya, Y. Iwata, K. Nishimura, and E. Yashima, *Angew. Chem. Int. Ed.*, **56**, 791 (2017).
35. J. M. Ren, J. Subbiah, B. Zhang, K. Ishitake, K. Satoh, M. Kamigaito, G. G. Qiao, E. H. H. Wong, and W. W. H. Wong, *Chem. Commun.*, **52**, 3356 (2016).
36. L. Zhang and A. Eisenberg, *J. Am. Chem. Soc.*, **118**, 3168 (1996).
37. M. Moffitt, H. Vali, and A. Eisenberg, *Chem. Mater.*, **10**, 1021 (1998).
38. S. N. Jaisankar, N. Haridharan, A. Murali, P. Sergii, M. Špírková, A. B. Mandal, and L. Matějka, *Polymer*, **55**, 2959 (2014).
39. P. Pereira, H. Gaspar, L. Fernandes, and G. Bernado, *Polymer Testing*, **47**, 130 (2015).
40. Y-P. Sun, B. Ma, C. E. Bunker, and B. Liu, *J. Am. Chem. Soc.*, **117**, 12705 (1995).
41. F. Cataldo, *Polym. Int.*, **48**, 143 (1999).
42. H. Kuzmany, R. Winkler, and R. Pichler, *J. Phys.: Condens. Matter*, **7**, 6601 (1995).